Met Office

Initial Implementation of an Inversion Technique for Estimating Volcanic Ash Source Parameters in Near Real time using Satellite Retrievals

Forecasting Research Technical
Report No: 604

17/12/2015

R. E. Pelley, M. C. Cooke, A. J. Manning,
D. J. Thomson, C. S. Witham and M. C. Hort

Abstract

When using dispersion models to predict the quantitative transport of volcanic ash, source term parameters defining the emission characteristics are required. Retrievals of ash column loadings can be calculated using data from satellite based instruments such as the SEVIRI (Spinning Enhanced Visible and Infrared Imager) instrument on-board the MSG (Meteosat Second Generation) satellite, offering insight into the volcanic ash plume. This paper describes a method for estimating the source term parameters using these satellite retrievals within an inversion modelling technique. This method has been available to the London Volcanic Ash Advisory Centre since February 2015 to assist with the provision of guidance. We introduce a framework which allows the inversion approach to be used during a volcanic eruption, providing source term parameter updates multiple times per day.

Our inversion technique applies a probabilistic approach, allowing the uncertainty in the satellite retrievals to be considered. Using Bayes theorem, a cost function to compare the satellite retrievals with the NAME model ash plume is derived. The minimum of this cost function provides the optimal source term parameters for simultaneously fitting the model ash loadings to the satellite retrievals and for fitting to *a priori* estimates of the emissions, taking account of the estimated errors in the retrievals and in the *a priori* emissions. An optimization algorithm, simulated annealing, is used to find this minimum. We discuss the considerations needed for the inversion framework to produce source term parameters in a timely manner during an eruption and test the approach using satellite retrievals from the 2010 Eyjafjallajökull and the 2011 Grímsvötn eruptions.

© Crown Copyright 2015

Contents

© Crown Copyright 2015

1 Introduction

The hazard posed by volcanic ash to aviation is well known (*Casadevall*, 1994). The London Volcanic Ash Advisory Centre (VAAC), hosted by the Met Office, is responsible for issuing volcanic advisories for the North-East Atlantic region. These advisories provide guidance to the aviation industry on the location and dispersion of volcanic ash.

Satellite products can be used to show the current extent of the volcanic clouds, whilst dispersion models such as NAME (Numerical Atmospheric-dispersion Modelling Environment) (*Jones et al.*, 2007) allow forecasters to predict the evolution of the volcanic ash. The accuracy of the dispersion models is affected by, among other contributing factors, the quality of the source term parameters which drive the model. This is particularly the case if trying to estimate ash concentrations rather than just the horizontal extent of the ash.

When modelling volcanic ash dispersion, source term parameters for the eruptive plume height, the mass release rate of ash and the vertical distribution of the ash within the eruptive plume are required. In regions such as Iceland, volcanoes are well monitored and estimates of the eruptive plume height can be made from radar and web cameras (*Arason et al.*, 2011; *Petersen et al.*, 2012b). These measurements are subject to uncertainties. The atmospheric conditions can add to this uncertainty as they can affect the position of maximum rise in strong winds.

Determining the mass release rate is more difficult; measurement techniques using remote sensing during an eruption are an active area of research (*Ripepe et al.*, 2013; *Marzano et al.*, 2013). Estimates of the mass release rate can be made using empirical relationships which relate the mass eruption rate to the eruptive plume height (*Mastin et al.*, 2009; *Sparks et al.*, 1997). These types of relationships tend to be an equation of best fit to data from many past eruptions. They give an estimate of the total mass eruption rate given the eruptive plume height. However, the relationships do not account for the mass eruption rate and eruptive plume height being affected by the strength of the prevailing wind (*Petersen et al.*, 2012a) and do not give the vertical distribution of ash resulting from the eruptive plume. One approach for the vertical distribution of ash is to approximate it to be uniform or more sophisticated techniques such as plume rise models can be used. Plume rise models can make use of information about the atmospheric conditions to estimate both the mass emission rate and the vertical spread of the erupting ash from the observed eruptive plume height (*Sparks et al.*, 1997; *Mastin*, 2007; *Devenish*, 2013; *Woodhouse et al.*, 2013).

An alternative approach is to estimate the source term parameters using satellite products. When coupled with a dispersion model and an inversion modelling technique the satellite products can be used to offer insight into the volcanic ash source term parameters (*Stohl et al.*, 2011; *Kristiansen et al.*, 2012). This has the potential to address the issues in determining the source term parameters, providing an alternative estimate of: the eruptive plume height; the mass eruption rate; and the vertical distribution of ash resulting from the eruptive plume.

This paper describes and demonstrates an inversion modelling technique which has been avail-

© Crown Copyright 2015

able to the London VAAC since February 2015 to assist with the provision of guidance. The method has been developed within InTEM (Inversion Technique for Emissions Modelling), the Met Office's inversion modelling system, to enable the estimation of volcanic ash source parameters. The satellite products, namely retrievals of ash column loadings produced using the scheme by *Francis et al.* (2012), are utilized within the inversion method. A dispersed ash plume, produced using NAME, is compared to the satellite retrievals via a cost function derived using a probabilistic approach. The inversion process then determines the source parameters which optimally fit the NAME plume to the satellite retrievals within their uncertainty (and, simultaneously, fit the emissions to *a priori* estimates of the emissions, again within their uncertainty).

There have been several other published approaches which apply inversion modelling to the finding of both the ash (*Stohl et al.*, 2011; *Kristiansen et al.*, 2012; *Schmehl et al.*, 2011; *Denlinger et al.*, 2012) and the SO_2 (*Boichu et al.*, 2013; *Seibert et al.*, 2011; *Eckhardt et al.*, 2008) source term parameters for volcanic eruptions. Most of these techniques produce the source terms post eruption. Here we present a methodology which allows the inversion technique to be used during a volcanic eruption. The methodology allows for source term parameter updates to be provided as more satellite retrievals become available. These new source parameters can be used in the dispersion model to give an updated dispersed ash plume prediction.

Discussed in this paper are the inversion modelling techniques applied within InTEM and the methodology for its use during a volcanic eruption. We discuss the considerations that need to be applied to the satellite retrievals, dispersion model and inversion technique so they can be used during an eruption. The capabilities of the methodology are then demonstrated using two test cases: the 2010 Eyjafjallajökull eruption; and the 2011 Grímsvötn eruption.

2 Satellite Retrievals

The Spinning Enhanced Visible and Infrared Imager (SEVIRI) on-board the geostationary Meteosat Second Generation (MSG) satellite is a 12 channel imager with four channels in the visible and eight in the infrared. At nadir the spatial resolution is 3 km for the infrared channels used for ash detection. At Icelandic latitudes ($\sim 65^\circ$) the pixels are of the order of 10 km. The instrument completes a full disc scan every 15 minutes.

Data from SEVIRI are used to retrieve volcanic ash physical properties using a 1-dimensional variational (1D-Var) analysis methodology detailed in *Francis et al.* (2012). The retrieval uses an optimal estimation technique to minimize a cost function to solve for the pressure of the ash layer (p_{ash}), ash column loading (L) and ash particle effective radius (R_{eff}) for each SEVIRI pixel. Analysis errors can be derived from the cost function allowing for errors in p_{ash}, L and R_{eff} to be estimated.

The ash column loading values (in $\mathrm{g m^{-2}}$) and associated errors are then re-gridded to 0.5625° longitude and 0.3750° latitude (approximately 40 km grid cells) and averaged temporally to one hourly files for use within InTEM. If over 50% of the pixels within a grid cell are flagged as ash then the cell is flagged as ash contaminated. The mean column loading values are calculated using all the pixels in a given cell (with zero assumed for non-flagged pixels) and with the column loading error values being evaluated by averaging the analysis errors for only those pixels flagged as ash.

Clear sky locations, which are free from both ash and meteorological cloud, can also be also used in InTEM. A satellite pixel is flagged as clear sky if there is no cloud identified based on the scheme described by *Hocking et al.* (2011) and no ash is detected using the scheme of *Francis et al.* (2012). If over 90% of the satellite pixels within a model grid cell are flagged as clear sky the model cell is flagged as clear sky and assigned a column loading of zero. The conservative minimum detection threshold is 0.5 gm^{-2} for the volcanic ash column loadings estimated from the method of *Francis et al.* (2012). This minimum threshold is dependent on the altitude of the plume and temperature profile of the atmosphere. The use of this minimum threshold means it is possible for locations containing less than 0.5 gm^{-2} of ash to be flagged as clear sky locations. Therefore an error of 0.5 gm^{-2} is assigned to the clear sky retrievals.

The creation of ash and clear sky retrievals using the above methods leads to two data-sets (ash and clear sky) with high confidence in the detection for each category. This means that some areas of ash and no-ash will be missed but allows us to use the data in an automated framework that could be used operationally during a volcanic eruption.

3 NAME

InTEM requires information on how erupted material could dilute downwind of a volcano. This is provided by NAME, a Lagrangian stochastic atmospheric dispersion model. Within NAME, model particles are tracked through a computational atmosphere using wind fields provided by a numerical weather prediction (NWP) model. The stochastic element adds random motions to the model particle trajectories, representing atmospheric turbulence. Model particles carry a mass of the dispersing substance defined by a source term. In our case the dispersing substance is volcanic ash. Sedimentation due to gravitational settling is modelled using a fall velocity related to the particle diameter and density. For volcanic ash a particle density of 2300 kg m^{-3} is assumed (*Devenish*, 2012; *Webster et al.*, 2012). Also modelled are deposition of particles due to precipitation (wet deposition) and non-sedimentation driven dry deposition involving the loss of particles due to diffusion to the surface (*Webster et al.*, 2012).

When modelling the dispersion of volcanic ash each model particle represents numerous real ash particles of a particular diameter. The particle diameters used are prescribed by a particle size distribution. We use a particle size distribution based on data given by *Hobbs et al.* (1991) and include diameters in the range 0.1 μm to 100 μm. This will not be the full range of particle diameters that will be emitted from the volcano, rather it is representative of the fine ash particle diameters that will undergo long range transport. Therefore, the NAME source term is defined as an effective source strength which represents the fine ash fraction of the total mass emitted from the

© Crown Copyright 2015

source (*Webster et al.*, 2012). Only modelling the fine ash fraction has computational advantages and is justified as larger particles are thought to fall out of the plume near to the volcano.

The effective source strength also accounts for any particles which may have combined due to aggregation following collisions with other particles. The aggregation process is thought to mostly occur near the volcano due to the high number of particles in this region (*Webster et al.*, 2012). NAME does not model aggregation processes and so the effective source strength assumes that all large aggregates (> 100 μm) have fallen near to the volcano.

For computational efficiency a particle life span of six days is assumed here but this could be changed. It is thought that most of the ash is removed from the atmosphere by natural processes by this time or the ash has become widely dispersed (*Webster et al.*, 2012). Therefore, concentrations of particles older than six days should be small.

NWP meteorological data from a variety of different numerical models can be used to drive NAME. For the NAME runs under the current test framework we make use of meteorological data from the global configuration of the Met Office's Unified Model (MetUM). The global data used here have a temporal resolution of three hours and a horizontal resolution of approximately 25 km in mid latitudes. The vertical grid consists of 75 unevenly spaced levels with a resolution of approximately 300-400 m in the mid-troposphere.

NAME source terms can be defined at any time and location (horizontal and vertical) and multiple sources can be used in a single NAME run. To allow InTEM to find time and height varying release rates we use multiple source terms released from the volcano location at different times and heights (a source term profile). InTEM will then attempt to select the best linear combination of these sources. To capture all variability in the source term profile, the individual sources are defined so that there are no gaps in time or height. Each source is assigned a nominal release rate of 1 g s^{-1}. The time and height intervals can be selected with any resolution, although finer resolutions require more computational resource. Figure 1 illustrates the multiple source term release for a single day in an eruption using a time interval of three hours and a height interval of 4 km with a total of six sources per time interval. The pattern of sources for a single day is repeated for all days in the eruption. The height interval and number of sources per time need to be selected so that the highest possible eruptive plume height is included in the NAME sources height range. For historical eruptions which have good observations of the eruptive plume this height is known. However, during an ongoing eruption an assumption of the highest plausible eruptive plume height needs to be made.

The concentrations resulting from the individual source terms are output hourly on a horizontal domain. The domain currently used covers part of the northern hemisphere from the East Canadian coastline to Eastern Europe. We are primarily concerned with Icelandic volcanic eruptions and hence the horizontal domain chosen. The horizontal grid covering this domain ranges from 60°W to 35°E and from 30°N to 80°N, with a resolution of 0.5625° longitude and 0.375° latitude. The grid and resolution are configured to coincide with the regridded satellite retrievals horizontal grid.

© Crown Copyright 2015

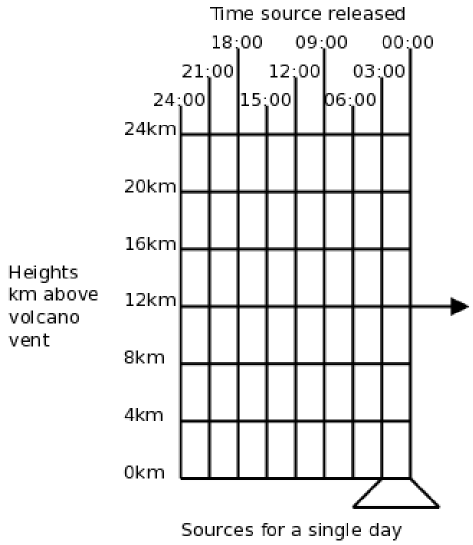

Figure 1: NAME source terms released at varying times and heights for a single day in an eruption. The same source term pattern applies to all days in an eruption. For this example the time interval is three hours and the height interval 4 km with six sources per time interval. The resulting concentrations are used to initialize InTEM.

Should InTEM need to be used for eruptions in other regions this domain and resolution can be changed although satellite retrievals would need to be available for that region.

The satellite data used in the inversion do not provide any information on the vertical distribution of the ash; they only give a total loading (gm^{-2}) for each of the horizontal grid cells. The ash concentrations from NAME need to be comparable to the satellite retrievals. To achieve this NAME integrates the concentrations over a 0-30 km vertical range returning a column loading. In addition, for a fair comparison between the model and satellite data sets, both need to represent the same particle size distribution. The distribution used in NAME represents a particle diameter range between 0.1 μm - 100 μm. This particle size range is larger than that detectable in the SEVIRI satellite retrievals, which has a detection range of approximately 1.0 μm - 30 μm (*Stohl et al.*, 2011). Figure 2 shows the distribution used in NAME and where the satellite retrieval size range overlaps. There is approximately 5% more mass in the NAME emissions than in the size range detectable by the satellite retrievals. To account for this larger proportion of mass in the NAME emissions and hence, at least near the source, in the NAME concentrations, the NAME concentrations are scaled down by 5% before use in InTEM. Should an alternative particle size distribution or alternative plume observations be used this proportion would need to be revised.

4 InTEM

The Met Office's inversion system (INTEM) was originally designed to estimate regional greenhouse gas emissions (*Manning et al.*, 2003, 2011; *Manning*, 2011). Recently this has been extended to add functionality to estimate volcanic ash source parameters using quantitative satellite retrievals.

© Crown Copyright 2015

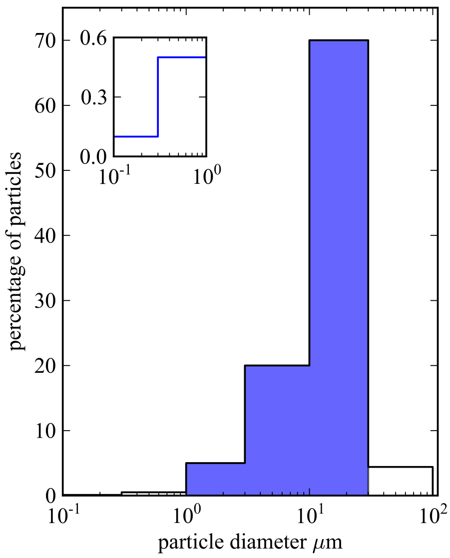

Figure 2: The particle size distribution based on the data given by *Hobbs et al.* (1991) used in the NAME runs. The shaded blue region indicates particle size range which is detectable in the satellite retrievals (1 μm to 30 μm). This range covers 95% of the distribution.

In terms of volcanic ash source parameters, the new estimates determined by InTEM provide a source term profile which can be used in dispersion models. The inversion technique in InTEM is capable of estimating a time and height varying source term profile which optimally fits both dispersion model plume concentrations to satellite retrievals of ash column loadings and model emissions to emission estimates based on the observed eruptive plume height. Although the satellite retrieval process provides estimates of ash pressure, ash column loadings and ash effective radius, InTEM currently only makes use of the ash column loading estimates (including clear sky locations).

This section describes the inversion technique used for volcanic ash source parameter estimation including: the use of *a priori* information and how it is estimated; the inversion modelling technique implemented in InTEM; and a method for using InTEM during an eruption.

4.1 *A priori* Source Term Profile

The inversion method within InTEM for volcanic ash source parameter estimation requires an initial best guess of the source term profile along with its uncertainty. The use of an *a priori* source term based on observed eruptive height prevents over-fitting to uncertain satellite observations, ensures optimal use is made of near source observations of the plume height and provides a guide to finding a more realistic solution. If only satellite observations are used, the inversion technique would find the source term which is the best mathematical fit to the observations; such best fit source term profiles may include emissions at heights above the observed eruptive plume height uncertainty. At locations where there is no ash or clear sky information, InTEM has no direct knowledge of the correct column loading. At these locations, in the absence of *a priori* information, a column

© Crown Copyright 2015

loading can only be inferred from the satellite retrievals at other times and locations, which may or may not give a suitable representation of the dispersed plume. When *a priori* information is used the inversion attempts to find a source term profile which fits within the uncertainty of both the observations and the *a priori*. This helps address the above issues and keep the column loadings resulting from the inversion source term profile within reasonable bounds.

To estimate an *a priori* for volcanic ash source term profiles we make use of the empirical relationship described by *Mastin et al.* (2009) and observations of the eruptive plume height. In principle it would be possible to regard the eruptive plume height observations as just more observations used in the inversion scheme. The *a priori* distribution would then need to be the distribution of volcano behaviours that we want to assume prior to any knowledge of observations of plume height. However, currently the use of *a priori* information is the only method for including the eruptive plume height observations within the inversion.

The Mastin relationship,

$$M = 140.84H^{1/0.241} \tag{1}$$

relates the eruptive plume height above the volcano vent H in km to a mass eruption rate for the volcano M in kg s^{-1}. The relationship is a power law best fit to many volcanic eruptions. We make use of M and H along with their uncertainty to produce a framework for estimating *a priori* source terms and an associated uncertainty.

An uncertainty for M can be estimated using the Mastin relationship 50% percentage interval. This indicates that 50% of cases fall within a factor of plus or minus four of M. There is also uncertainty in the observed eruptive plume heights. Well monitored volcanoes such of those in Iceland have eruptive plume heights estimated by several sources including web-cams and radar (*Arason et al.*, 2011; *Bjornsson et al.*, 2013); these will be subject to an uncertainty. To capture the uncertainty in H, a height error H_ϵ can be assigned to give minimum and maximum eruptive plume heights as

$$\begin{aligned} H_{min} &= H - H_\epsilon \\ H_{max} &= H + H_\epsilon \end{aligned} \tag{2}$$

Coupling the minimum and maximum heights with the Mastin relationship uncertainties gives estimates of a range for M as

$$\begin{aligned} M_{min} &= 35.21(H_{min})^{1/0.241} \\ M_{max} &= 563.36(H_{max})^{1/0.241} \end{aligned} \tag{3}$$

where M, M_{min} and M_{max} give total mass eruption rates covering the full particle size range of ash emitted from the volcano. Here within NAME we only model the transport of fine ash by using an effective source strength. In accordance with this the *a priori* source term profile is assumed to

© Crown Copyright 2015

be 5% of that given by the Mastin relationship (*Webster et al.*, 2012). This gives a framework for estimating an *a priori* effective source strength and its uncertainty for each observed eruptive plume height as

$$\begin{aligned} m &= 7.042H^{1/0.241} \\ m_{min} &= 1.760(H_{min})^{1/0.241} \\ m_{max} &= 28.168(H_{max})^{1/0.241} \end{aligned} \tag{4}$$

where m is the effective source strength and m_{min} and m_{max} its approximated minimum and maximum. To illustrate the use of this framework in approximating an *a priori*, Figure 3 shows the *a priori* value and its approximated ranges for an eruptive plume height of $H = 7.5$ km with an error of $H_\epsilon = 2.5$ km. Note that the calculated masses give no indication of the vertical spread over the eruptive plume height. For the *a priori* profile a uniform vertical spread of emissions are assumed.

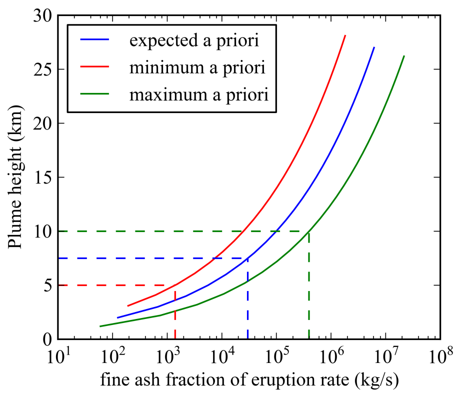

Figure 3: 5% of the mass eruption rate given by the Mastin relationship and its 50% prediction interval. The dashed lines show the masses for an example measured eruptive plume height of $H = 7.5$ km with a height error of $H_\epsilon = 2.5$ km.

The process for approximating the *a priori* value is repeated for each observed eruptive plume height. The times and heights of the *a priori* sources need to be remapped to fit the resolution of the NAME run source term profile. Therefore the masses are uniformly spread up to the height of the eruptive plume and are then averaged in time and height over each of the individual NAME sources. The same is done for the minimum and maximum values, producing an uncertainty range for each of the individual sources.

The *a priori* uncertainty framework in equation (4) attempts to incorporate an uncertainty in the prior effective source strengths. It does not incorporate uncertainty in the fine ash fraction. However, the ranges produced by this framework are thought to be large enough for InTEM to find a suitable source term profile.

© Crown Copyright 2015

4.2 The Inversion Technique

The inversion technique implemented in InTEM for approximating volcanic ash source parameters firstly requires the model column loadings for the individual source elements (produced using NAME) to be related to the satellite retrievals of both ash and clear sky locations. This can be done by forming a 'model observation'. A model observation o_{mi}, at location (x, y) and time t can be found given the model column loadings and the source term profile by using

$$\begin{aligned} o_{mi} =& c_{i,1}(x,y,t)e_1 + c_{i,2}(x,y,t)e_2 \\ &+ \cdots + c_{i,n}(x,y,t)e_n \end{aligned} \tag{5}$$

where o_{mi} is the ith model observation of column loading ($i = 1, 2, \ldots, k$), k is the total number of observations, $c_{i,j}$ is the column loading resulting from the jth model source at the same location and time (x, y, t) as the ith observation, e_j is the jth source term ($j = 1, 2, \ldots, n$) and n is the total number of model sources. This gives a system of equations,

$$\mathbf{Me} = \mathbf{o}_m \tag{6}$$

where **M** is the matrix of the model column loadings ($c_{i,j}$), named the source term dilution matrix, **e** is the vector of n source terms in the source term profile and $\mathbf{o}_m$ is the vector of k model observations.

The goal of the inversion technique is, by altering **e**, to find model observations which are an optimal fit to the satellite retrievals, $\mathbf{o}_a$. To allow the inversion technique to account for the uncertainty in the satellite retrievals and to address the issue of **M** rarely being invertible, InTEM uses a probabilistic approach to find **e**. Bayesian analysis and Gaussian probability distributions are used to produce a cost function, similarly to the approaches described by *Eckhardt et al.* (2008); *Tarantola* (2005); *Menke* (1989); and *Rodgers* (1976). The minimum of the cost function will give the **e** which is the optimal fit to the satellite retrievals and the *a priori* source term profile. InTEM uses the optimization technique simulated annealing to find this minimum.

Bayes theorem states:

$$P(\mathbf{e}|\mathbf{o}_a) = \frac{P(\mathbf{o}_a|\mathbf{e})P(\mathbf{e})}{P(\mathbf{o}_a)} \tag{7}$$

where $P(\mathbf{o}_a|\mathbf{e})$ is the probability density of getting the satellite retrieval ($\mathbf{o}_a$) given a source term profile **e**. $P(\mathbf{e})$ is the *a priori* probability density of **e**. The *a posteriori* (solution) probability, $P(\mathbf{e}|\mathbf{o}_a)$, is the probability density of the emissions given the satellite retrievals i.e. the inverse problem we are trying to solve. $P(\mathbf{o}_a)$ does not depend on **e**, therefore, $P(\mathbf{o}_a)$ is just a normalization constant. Then by Bayesian inference the *a posteriori* probability is proportional to the product of the probabilities of $\mathbf{o}_a$ given **e** and the *a priori* (*Yee*, 2008),

$$P(\mathbf{e}|\mathbf{o}_a) \propto P(\mathbf{o}_a|\mathbf{e})P(\mathbf{e}) \tag{8}$$

© Crown Copyright 2015

In terms of probability distributions the *a posteriori* with the highest probability density can be determined from the probability density $P(\mathbf{o}_a|\mathbf{e})P(\mathbf{e})$. To find the maximum, probability distributions for the satellite retrievals and *a priori* data are needed. For convenience we assume Gaussian distributions. The probability of getting the satellite column loadings given the emissions (**e**) is proportional to:

$$P(\mathbf{o}_a|\mathbf{e}) \propto \exp\left[-\frac{1}{2}\left(\mathbf{Me}-\mathbf{o}_a\right)^{\mathrm{T}}\mathbf{R}^{-1}\left(\mathbf{Me}-\mathbf{o}_a\right)\right] \quad (9)$$

and the *a priori* probability of the emissions (**e**) is proportional to:

$$P(\mathbf{e}) \propto \exp\left[-\frac{1}{2}\left(\mathbf{e}-\mathbf{e}_{ap}\right)^{\mathrm{T}}\mathbf{B}^{-1}\left(\mathbf{e}-\mathbf{e}_{ap}\right)\right] \quad (10)$$

where $\mathbf{e}_{ap}$ is the mean of the *a priori* probability distribution of emissions estimated as in section 4.1. **R** is the error covariance matrix for the satellite retrievals and the transport model. **B** is the error covariance matrix for the *a priori* source term profile. Combining these two probabilities using Bayes theorem gives the probability of the source term profile given the satellite retrievals (the inverse problem we wish to solve):

$$\begin{aligned}P(\mathbf{e}|\mathbf{o}_a) \propto \exp\Bigg[&-\frac{1}{2}\left(\mathbf{Me}-\mathbf{o}_a\right)^{\mathrm{T}}\mathbf{R}^{-1}\left(\mathbf{Me}-\mathbf{o}_a\right)- \\ &\frac{1}{2}\left(\mathbf{e}-\mathbf{e}_{ap}\right)^{\mathrm{T}}\mathbf{B}^{-1}\left(\mathbf{e}-\mathbf{e}_{ap}\right)\Bigg]\end{aligned} \quad (11)$$

Then taking the log of the above expression allows the maximum likelihood point to be found as the minimum of

$$\begin{aligned}J(\mathbf{e}) = &\left(\mathbf{Me}-\mathbf{o}_a\right)^{\mathrm{T}}\mathbf{R}^{-1}\left(\mathbf{Me}-\mathbf{o}_a\right) \\ &+\left(\mathbf{e}-\mathbf{e}_{ap}\right)^{\mathrm{T}}\mathbf{B}^{-1}\left(\mathbf{e}-\mathbf{e}_{ap}\right)\end{aligned} \quad (12)$$

This is known as the cost function. The **e** which gives the minimum value for J is the most likely solution to the inverse problem and will have the optimal fit to the satellite retrievals and to the *a priori* source term profile.

The Gaussian assumption creates a simple cost function and also has the property that the *a posteriori* distribution will also be Gaussian. This assumption allows negative values to be included in the uncertainty range which is not physically realistic. The avoidance of negative values in the *a posteriori* emissions is handled by the simulated annealing minimization scheme (see below), which searches for the cost function minimum under the constraint that all elements of **e** are non-negative. The Gaussian approach combined with this constraint therefore produces suitable *a posteriori* profiles.

The observation error covariance matrix **R** is a $k \times k$ diagonal matrix containing the satellite retrieval variances. We have assumed that there is no error in the transport model and for computational efficiency and convenience the satellite retrievals are assumed independent. Similarly the diagonals of **B** are filled with the variances of the *a priori* to give a $n \times n$ diagonal matrix. Again for computational efficiency and convenience the prior source terms are assumed to be independent and the covariances are set to zero. A variance for each *a priori* source term is approximated from the range as

$$(\sigma_j^a)^2 = \left(\frac{(e_{apmax})_j - (e_{apmin})_j}{7.6}\right)^2 \tag{13}$$

where $(e_{apmax})_j$ is the jth maximum *a priori* source term, $(e_{apmin})_j$ is the jth minimum *a priori* source term and $(\sigma_j^a)^2$ is the variance of the jth *a priori* source term. This approximation is based on 99.99% of values falling within plus or minus 3.8 standard deviations for a Gaussian distribution.

The advantage of assuming Gaussian uncertainties and a linear forward model is that the *a posteriori* distribution is also Gaussian. The error covariance matrix, **A**, for **e** can then be found from the second derivative of J,

$$\mathbf{A} = \left(\mathbf{M}^{\mathrm{T}}\mathbf{R}^{-1}\mathbf{M} + \mathbf{B}^{-1}\right)^{-1} \tag{14}$$

The diagonals of **A** can be interpreted as the variances of **e** giving a measure of the uncertainty in the solution. As mentioned previously the Gaussian assumption is flawed as it could include negative values in the uncertainty. This also applies to the *a posteriori* **e**, and its uncertainties. There is some uncertainty in the precise interpretation of A because of the negatives included in the Gaussian assumptions. As a result it is more appropriate to regard the variances in **A** as an indicator of the uncertainty in the solution for **e**. Smaller variances indicate less uncertainty, larger variances more uncertainty. The variances are therefore useful as a comparative measure of the uncertainty between two solutions.

To solve the inverse problem, InTEM uses the optimization technique simulated annealing to find the minimum of the cost function, equation (12). The particular variant of simulated annealing applied is described by *Press et al.* (1992). Simulated annealing is an iterative method which begins by defining an initial set of $n+1$ solutions which span the full range of possible solutions. To determine this range we use the *a priori* source term profile and its uncertainty range to give a framework for creating the initial solution set as

$$\begin{aligned} \mathbf{S}^0 &= \mathbf{e}_{apmin} \\ \mathrm{S}_i^j &= \begin{cases} (e_{apmin})_i & \text{if } i \neq j \\ (e_{apmax})_i & \text{if } i = j \end{cases} \end{aligned} \tag{15}$$

where $i, j = 1, 2, \ldots, n$ and S_i^j is the ith component of the jth solution in the solution set. $\mathbf{e}_{apmin}$ is the minimum *a priori* source term profile and $(e_{apmin})_i$ is the ith component of the minimum *a priori* source. Similarly $(e_{apmax})_i$ is the ith component of the maximum *a priori* source.

The costs for each of the $\mathbf{S}^r$, $r = 0, 1, \ldots, n$, are calculated using equation (12). In each iteration the solution with the worst cost is modified by: reflecting about the average solution; extrapolating from the average; or contracting about the average. This continues until either the minimum is

© Crown Copyright 2015

found, indicated by all solutions converging to a similar cost, or the maximum number of iterations are exceeded.

Simulated annealing is a global optimization technique and to prevent the algorithm from only approaching a local minimum a random fluctuation is added to each of the costs. Therefore in some cases the true worst solution is not selected for modification, allowing movement away from a local minimum. The random fluctuation is based on a 'temperature' which is gradually reduced. This acts to decrease the random fluctuation as the algorithm approaches a solution. The temperature, T, is calculated via the temperature schedule,

$$T = \left(1.0 - \frac{k}{k_{max}}\right)^2 \tag{16}$$

where k is the number of elapsed iterations at the point of calculating the temperature and k_{max} is the maximum number of iterations. Further details of the simulated annealing algorithm are given in *Press et al.* (1992) (pp. 443-447). Any new solutions are adjusted to prevent negative emissions. Simulated annealing has the ability to use any cost function.

4.3 Using InTEM during an eruption

InTEM can be used during an eruption if embedded in an appropriate framework. The framework developed at the Met Office is designed to produce source term profile estimates every six hours (the source term profile update frequency) and is automated; this duration can be changed if required.

To solve the inverse problem three data sets are required: the source term dilution matrix; satellite retrievals; and an *a priori* source term profile. The source term dilution matrix is produced using NAME with the latest MetUM analysis meteorological data. The satellite retrievals are routinely produced and are readily available for use. The *a priori* source term profile is produced using the latest observations of the eruptive plume heights available to the London VAAC.

To summarize, the steps taken by the system to estimate source term profiles during an eruption are as follows:

1. Run NAME with the latest meteorology valid until a defined time, *t*. (Ideally analysis meteorology is used, but short period forecasts can be used instead when the analysis is not yet available.)

2. Create an *a priori* source term profile using all observed eruptive plume heights from the start of the eruption until *t*.

3. Run InTEM to estimate a new source term profile given all available satellite retrievals from the start of the eruption until *t*.

4. Repeat the process every six hours.

© Crown Copyright 2015

In practice there will be a delay between obtaining the new source term profile and real time. This is due to two factors, the need to wait for the satellite retrievals and the time it takes to complete the above steps.

To enable InTEM to produce regular source term updates during an eruption its computational efficiency needs to be addressed. The computational effort required by InTEM is mainly governed by the resolution of the source term profile, the number of satellite retrievals and the length of the eruption. More satellite retrievals and sources (caused by finer resolutions or longer eruptions) creates a larger dilution matrix $\mathbf{M}$ and larger vectors $\mathbf{e}$ and $\mathbf{o}_a$, therefore requiring more effort to calculate the cost using equation (12).

Several steps have been taken to improve the computational efficiency of InTEM. These include: the parallelisation of parts of the code base; only solving for satellite retrievals that lie at the same location as the NAME plume (InTEM cannot fit to a satellite retrieval at a location where there are no dilution concentrations); discarding all sources which are above the observed eruptive plume height plus its height error from the inversion calculations (these sources will always be set to zero by InTEM when using the current *a priori* framework); and selecting the source term profile resolution to be 3 hours by 4 km in height with a maximum eruptive plume height of 24 km above the volcano vent. The source term time resolution (3 hours) must be a factor of the source term profile update frequency (6 hours). Sensitivity tests for two test cases, the 2010 Eyjafjallajökull and 2011 Grímsvötn eruptions, have shown that suitable results can be produced using this resolution. However, the resolution and top height can be changed when necessary. In addition to these steps the use of more efficient optimisation techniques to minimize the cost function, equation (12), could be investigated.

5 Results

The inversion framework for use during a volcanic eruption can be tested using historical cases provided satellite retrievals, meteorological data and observed eruptive plume heights are available for the eruption. These data are available for both the 2010 Eyjafjallajökull and 2011 Grímsvötn eruptions. As previously described the current framework will produce a new source term profile every six hours. Source term profiles will be estimated at regular intervals, using satellite retrievals until 00:00, 06:00, 12:00, and 18:00 on each day. Therefore, with the exception of the first source term profile, due to an eruption potentially starting mid-interval, each new profile will use an extra six hours of satellite retrievals. The framework is tested using both of the afore mentioned test cases, demonstrating the benefits of using the inversion technique and discussing the variability in the source term profile as the data cut-off time advances.

© Crown Copyright 2015

5.1 Eyjafjallajökull

The Icelandic volcano Eyjafjallajökull erupted on the 14th of April 2010 at 09:00 UTC. The volcano is located at 63.63°N, 19.62°W and has a vent height of 1666 m asl. The eruption lasted 39 days, ending on the 23rd of May 2010 at 18:00. *Gudmundsson et al.* (2012) have characterized the eruption into four distinct phases: 1: 14-18 April, the first explosive phase; 2: 18 April - 4 May, the low discharge mainly effusive phase; 3: 5 May - 17 May, the second explosive phase; and 4: 18 - 22 May the declining phase. The strong northwesterly winds (*Petersen*, 2010) and length of the eruption meant that major disruption was caused to aviation through and within European air space.

To use the inversion framework, satellite retrievals and eruptive plume heights, for producing *a priori* profiles, are required for the entire duration of the eruption. Eruptive plume heights were provided in real time to the London VAAC from the Icelandic Met Office during the eruption. They are an interpretation of the readings from the radar at Keflavík airport (*Arason et al.*, 2011) and other observations. The heights shown in Figure 4, are a post eruption revision which only used local Icelandic observations and do not incorporate satellite data (*Webster et al.*, 2012) and are used to calculate the *a priori* source term profile. To calculate the uncertainty in the *a priori* an eruptive

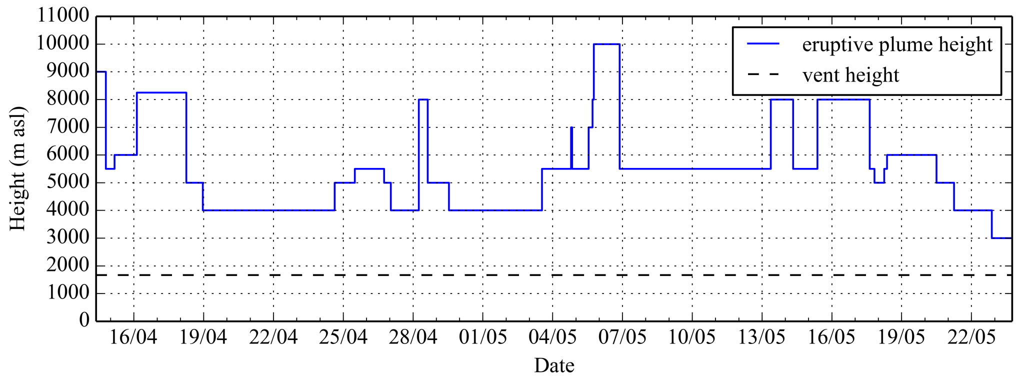

Figure 4: Eruptive plume heights for the Eyjafjallajökull 2010 eruption estimated from local observations.

plume height error of H_ϵ = 2000m is assumed so that $H_{min} = H - 2000$ and $H_{max} = H + 2000$. This is selected to allow a reasonable amount of variability in the *a priori* eruptive plume heights. Satellite retrievals of both ash and clear sky have been processed using SEVIRI data from the start of the eruption until 29/05/2010 23:00 UTC. The satellite retrievals extend after the eruption has ceased to allow for any remaining ash in the atmosphere to be included in the inversion. Using the inversion framework to produce source term profiles every six hours will result in a total of 184 source term profiles (4 source term profiles a day for 46 days). Each of these source term profiles will contain individual sources with a three hourly time resolution and a 4 km height resolution.

Due to the length of the 2010 Eyjafjallajökull eruption an example has been selected from the second half of the eruption, phases three and four. For these two phases more ash satellite retrievals are available for use by InTEM allowing a greater impact in the inversion results to be

© Crown Copyright 2015

demonstrated. Figure 5 shows four of the source term profiles produced for the eruption compared to the *a priori* source. Each source term profile uses an extra six days of satellite retrievals than

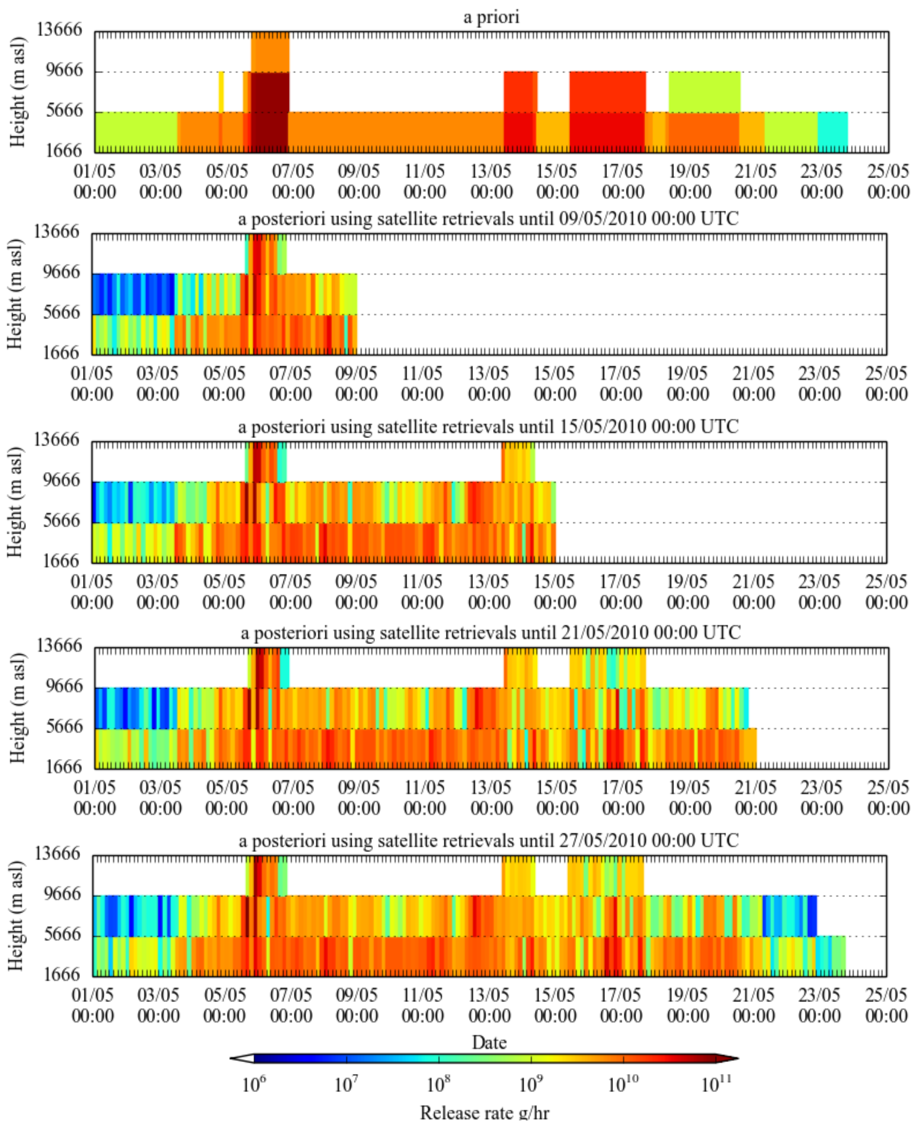

Figure 5: Source term profiles produced from InTEM compared to the *a priori* for the final two phases of the 2010 Eyjafjallajökull eruption. Each inversion source term profile uses six days more of satellite retrievals than the previous one.

the previous one. These source terms do not show the release rates for dates prior to 01/05/2010. Figure 6 shows the plumes from each *a posteriori* source term compared to the *a priori* and satellite retrievals for the 06/05/2010 17:00 – 18:00 UTC. Note that the satellite ash column loading image does not show any uncertainties. The example demonstrates the effect of including more satellite retrievals (providing more information about the ash plume) in the inversion. All satellite retrievals used in the inversion have an effect on the optimal fit; as more satellite retrievals are used the optimal fit changes. For all the *a posteriori* source term profiles shown in Figure 5 the satellite retrievals of ash column loadings act to reduce the resulting column loadings when compared to the *a priori* (see Figure 6). As more satellite retrievals are included the later retrievals have the effect of further

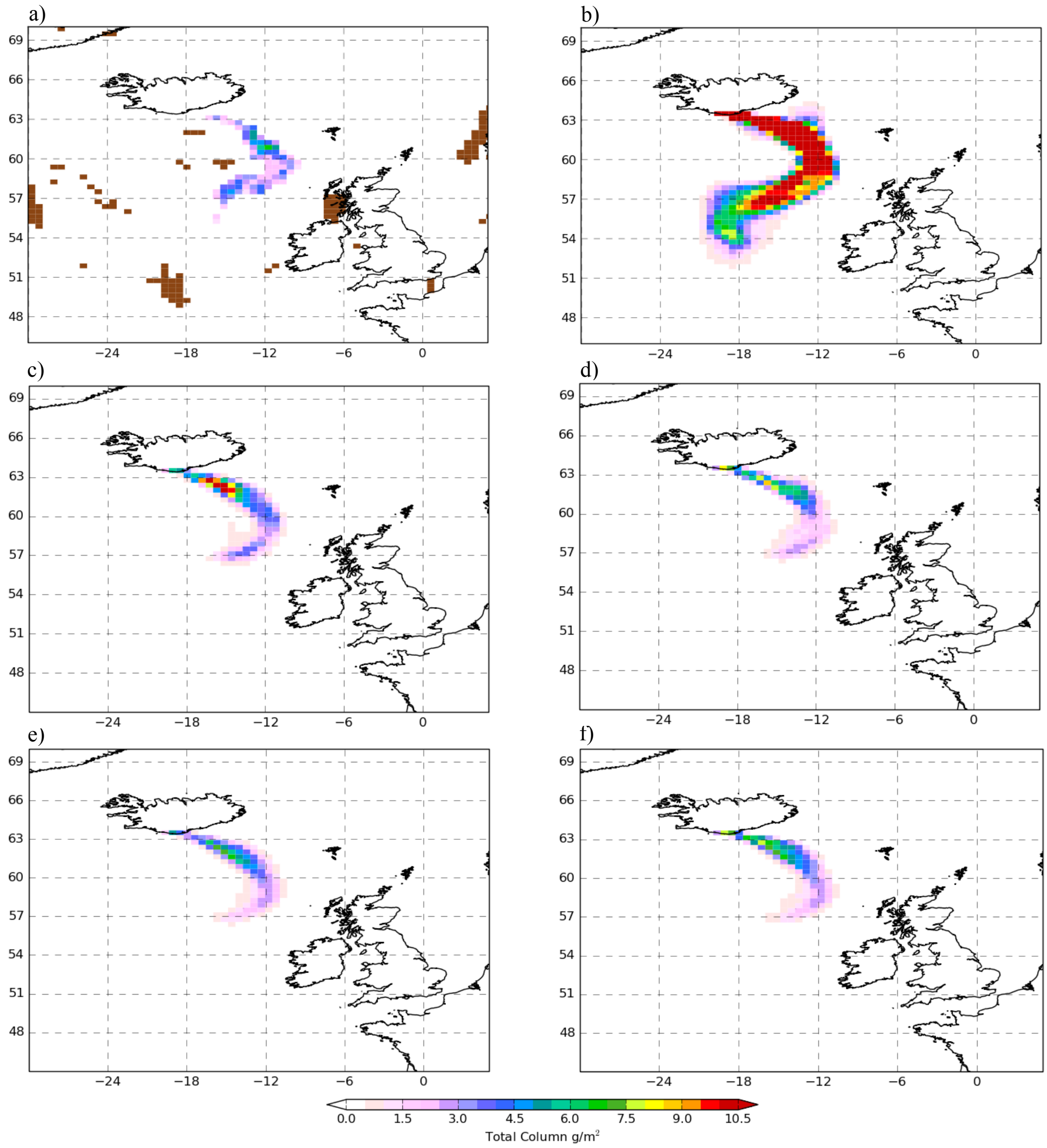

Figure 6: Plumes for the hour between 06/05/2010 17:00 and 06/05/2010 18:00 UTC for the 2010 Eyjafjallajökull eruption using the source term profiles given in Figure 5 compared to the satellite retrievals for the same hour. a) The satellite retrievals with clear sky retrievals shown in brown. b) The *a priori* plume. c) The *a posteriori* plume resulting from the profile using satellite retrievals until 09/05/2010 00:00 UTC. d) The *a posteriori* plume resulting from the profile using satellite retrievals until 15/05/2010 00:00 UTC. e) The *a posteriori* plume resulting from the profile using satellite retrievals until 21/05/2010 00:00 UTC. f) The *a posteriori* plume resulting from the profile using satellite retrievals until 27/05/2010 00:00 UTC.

reducing the column loadings as the inversion tries to find the new optimal fit.

The inversion process only makes use of satellite retrievals which lie at the same locations as the dilution matrix concentrations. During the first half of the eruption very few ash retrievals were co-located with the dilution matrix concentrations. This is because of the presence of ice cloud above the ash preventing the detection by SEVIRI. The lack of ash retrievals means any identified clear sky locations will dominate in the inversion process. If there are co-location errors in the NAME dilution concentrations i.e. NAME places mass where the satellite retrievals say there is none, then

© Crown Copyright 2015

without other ash column loading information the inversion approach will reduce the volcano release rates. Allowance for co-location errors could potentially be included in the inversion approach either via the use of an ensemble of meteorological data or by including an approximation of the transport model uncertainty.

5.2 Grímsvötn

The Icelandic volcano Grímsvötn erupted on the 21st of May 2011 at 19:13 UTC. The volcano is located at 64.42°N, 17.33°W and has a vent height of 1725 m asl. The eruption lasted for approximately four days and ended on the 25th of May 2011 at 02:30 UTC. Satellite retrievals of both ash column loadings and cloud free regions have been processed using SEVIRI data from the 21/05/2011 19:00 UTC until the 29/05/2011 18:00 UTC. The use of satellite retrievals up to the 29/05/2011 18:00 UTC, after the volcano has finished erupting, allows any ash detected by the retrievals remaining in the atmosphere to be used in the inversion.

Similarly to the Eyjafjallajökull eruption, eruptive plume heights were provided in real time to the London VAAC from the Icelandic Met Office during the eruption. These heights, shown in Figure 7, are used to calculate the *a priori* source term profile. The uncertainty in the *a priori* eruptive plume height is also assumed to be plus or minus 2000m ($H_\epsilon = 2000$).

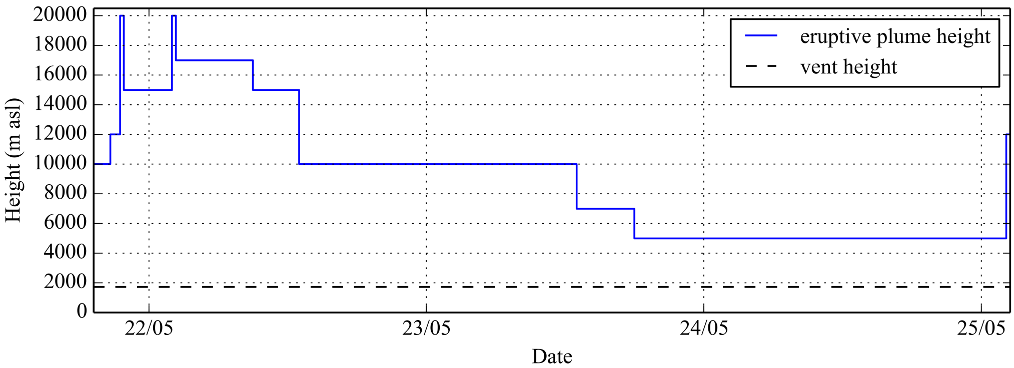

Figure 7: Eruptive plume heights for the Grímsvötn 2011 eruption estimated from local observations.

The 2011 Grímsvötn eruption presents an interesting test case for the inversion system. Wind shear led to most of the upper plume being transported north of Iceland and the lower plume being transported to the south. This occurred during the initial stages of the eruption when the 20 km eruptive plume heights were reported. Using an *a priori* which places ash uniformly up to the top of the eruptive plume heights will give a modelled plume with ash transport to the north and south of Iceland. The satellite retrievals do not support this prediction and show very little ash north of Iceland (*Cooke et al.*, 2014). It is thought that the upper section of the plume contained mostly SO_2 and ash was principally present in the lower section. This led to mostly SO_2 being transported north rather than ash. The inversion system should be able to correct the modelled column loadings and find an ash source term profile which fits the dispersed plume to the satellite retrievals.

© Crown Copyright 2015

Using all the available satellite retrievals in the inversion framework will allow for the production of 32 (4 a day for 8 days) source term profiles throughout the eruption. Figure 8 shows how these source terms evolve in the rolling framework, with four source term profiles selected and compared to the *a priori*. In all cases there is a large reduction in mass when compared to the *a priori*. There

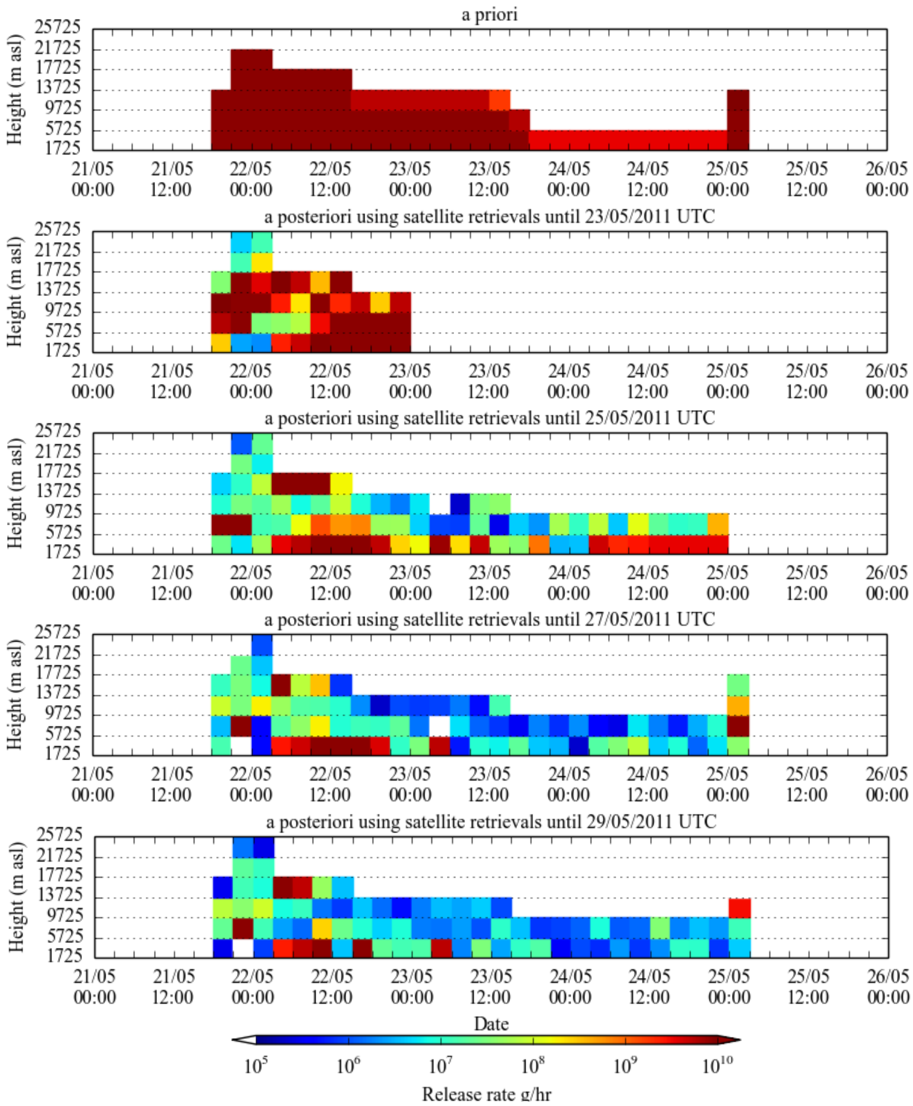

Figure 8: Source term profiles produced from InTEM compared to the *a priori* for the Grímsvötn 2011 eruption at various stages in the eruption. Each inversion source term profile uses two days more of satellite retrievals than the previous one. The eruption ceased on the 25/05/2011 at 02:30. Any release rates in the source term profile past this time will be zero. The source term profiles make use of satellite retrievals past this time.

is much variability in the early source terms within the profiles. This variability is reduced as the cost function forces a particular fit to the satellite retrievals. In some cases the uncertainty in the satellite retrievals may allow the optimal fit to continually vary.

The source term profiles in Figure 8 can be used in NAME to give a prediction of the spread of the ash plume. Figure 9 shows the NAME plumes from each of the five sources term profiles compared to the satellite retrievals for the hour between 22/05/2011 23:00 and 23/05/2011 00:00.

© Crown Copyright 2015

The *a priori* plume shows large differences for the satellite retrievals and largely over-estimates the

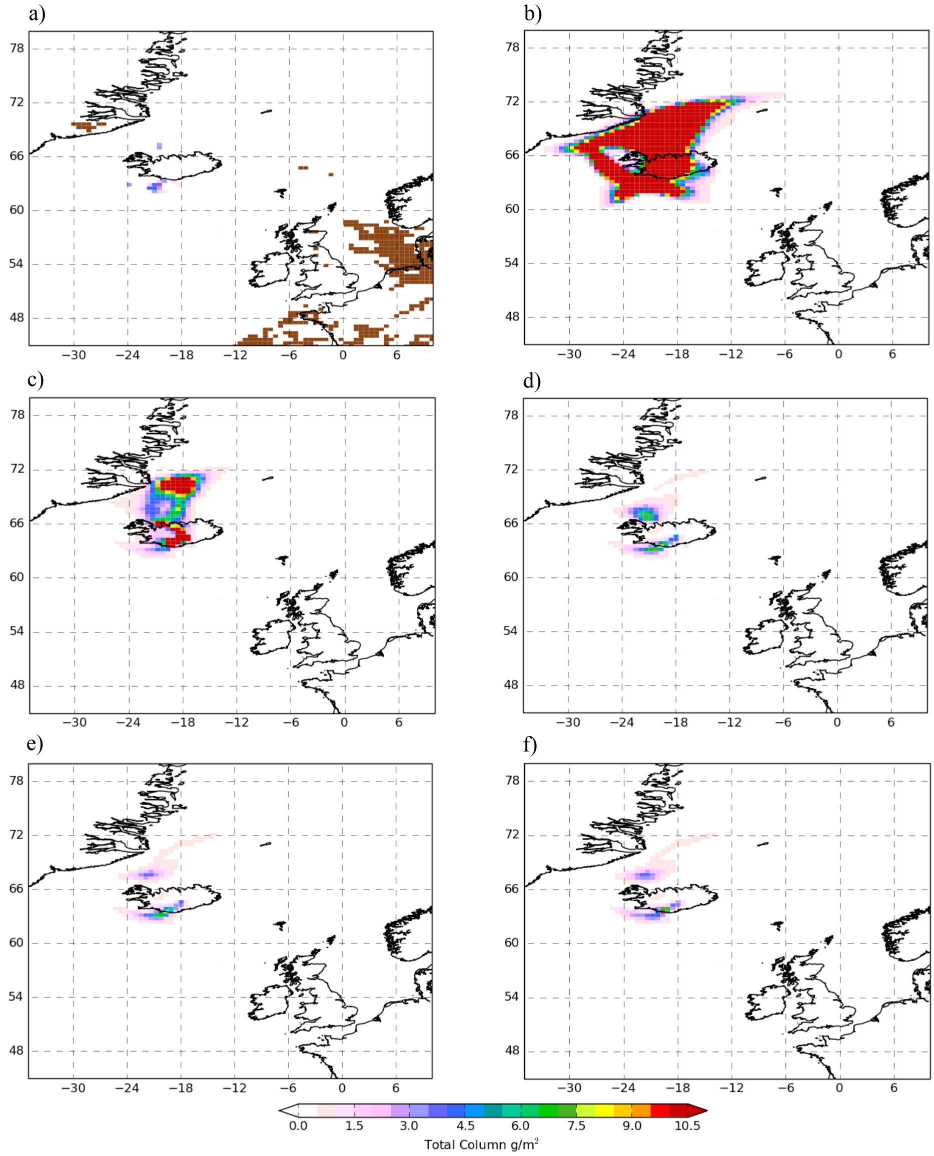

Figure 9: Plumes for the hour between 22/05/2011 23:00 and 23/05/2011 00:00 UTC for the Grímsvötn eruption using the source term profiles given in Figure 8 compared to the satellite retrievals for the same hour. (a) The satellite retrievals with clear sky locations shown in brown; (b) Plume when using the *a priori* source term profile; (c) Plume resulting from the *a posteriori* profile using satellite retrievals until 23/05/2011 00:00 UTC; (d) Plume resulting from the *a posteriori* profile using satellite retrievals until 25/05/2011 00:00 UTC; (e) Plume resulting from the *a posteriori* profile using satellite retrievals until 27/05/2011 00:00 UTC; (f) Plume resulting from the *a posteriori* profile using satellite retrievals until 29/05/2011 00:00 UTC.

magnitude and spread of the plume, particularly to the north of Iceland, when compared to all of the inversion source term profiles. All the inversion source term profiles fit reasonably well compared to the satellite retrievals. It should be noted that any white areas on the satellite retrievals image (Figure 9a) indicate that there is no information about the plume at this time and location, although the plume predictions at these locations using the inversion source term profiles are influenced by satellite retrievals at other times and locations. In these areas plume magnitude and spread

© Crown Copyright 2015

vary between source term profiles. As more satellite retrievals become available, providing more knowledge about the spread of the plume, the early source terms are changed to provide a better fit to the satellite retrievals. However, they will still be constrained by the uncertainty of the earlier retrievals and hence the plume at the same location as the satellite retrievals does not vary greatly. Figure 9a does not show the uncertainty in the satellite retrievals. In many cases the uncertainty is as large as the satellite retrieval itself and a zero column loading can be within this uncertainty.

The inversion profiles in Figure 8 correctly reduce the large amount of ash seen to the north in the *a priori* plume in Figure 9. Some of this correction is caused by later satellite retrievals which provide more cloud free regions to the north. During an eruption the first information provided by InTEM would be that in Figure 9c. This shows the plume prediction that would have been possible using the *a posteriori* source term profile during an eruption. Although this test case shows that the inclusion of more satellite retrievals further effects the *a posteriori* plumes, the plume in Figure 9c still offers a better fit to the satellite retrievals than the *a priori*.

6 Conclusions

We have demonstrated a method for estimating volcanic ash source parameters in an automated manner during a volcanic eruption. The method uses satellite retrievals from the SEVIRI instrument of ash column loading and of cloud free locations and dispersion information from NAME, with the InTEM inversion modelling system embedded in a suitable framework. The detection limit for the satellite retrievals is conservative to avoid false alarms, allowing the data to be used without human intervention.

The inversion modelling technique applied in InTEM uses a probabilistic approach and an optimization method to solve the inverse problem. The probabilistic approach is advantageous as it allows uncertainties in the satellite retrievals, *a priori* emissions and *a posteriori* emissions to be mathematically addressed. Combining this probabilistic approach with the simulated annealing optimization algorithm avoids finding negative values in the solution.

To allow the inversion approach to be used during a volcanic eruption InTEM has been embedded in a framework which gives automated updates to the source term parameters multiple times a day as more satellite retrievals become available. It has been tested using data from the 2010 Eyjafjallajökull and the 2011 Grímsvötn eruptions. The updated source term estimates enable the generation of new model information on the ash cloud extent and its column loadings. The source parameters from the most recent inversion calculation offer the optimal fit to all the satellite retrievals used and to the *a priori* source term profile. This optimal fit changes as more satellite retrievals become available.

In both of the test cases the inversion approach offers insight into the required volcanic ash source parameters as the eruption progresses. The column loadings resulting from the *a posteriori* source parameters are distinctly different to the column loadings generated using the *a priori* solu-

© Crown Copyright 2015

tion for both test cases. There are some time instances where the optimal fit given by the inversion source term parameters may not improve over the prior. This is expected; there are uncertainties in the satellite retrievals and we have not considered the transport model uncertainty.

The InTEM results demonstrate an automated approach in using satellite information to inform the dispersion model predictions. This inversion capability combined with other volcanic ash evidence, such as other satellite imagery and non-satellite observations, should provide valuable insight into volcanic ash plume dispersion and assist with the provision of advice.

Acknowledgments

The authors would like to thank staff at the Icelandic Meteorological Office for providing the eruptive plume heights for both test cases demonstrated in the paper.

References

Arason, P., G. N. Petersen and H. Bjornsson (2011), Observations of the altitude of the volcanic plume during the eruption of Eyjafjallajökull, April-May 2010, *Earth Syst. Sci. Data*, *3*, 9-17, doi:10.5194/essd-3-9-2011.

Bjornsson, H., S. Magnusson, P. Arason and G. N. Petersen (2013), Velocities in the plume of the 2010 Eyjafjallajökull eruption, *J. Geophys. Res.*, *118*, 11698-11711, doi:10.1002/jgrd.50876.

Boichu, M., L. Menut, D. Khvorostyanav, L. Clarisse, C. Clerbaux, S. Turquety and P.-F. Coheur (2013), Inverting for volcanic SO2 flux at high temporal resolution using spacebourne plume imagery and chemistry-transport modelling: the 2010 Eyjafjallajökull eruption case study, *Atmos. Chem. Phys.*, *13*, 8569-8584, doi:10.5194/acp-13-8569-2013.

Casadevall, T. J. (1994), The 1989-1990 eruption of Redoubt Volcano, Alaska: impacts on aircraft operations, *J. Volcanol. Geotherm. Res.*, *62*, 301-316.

Cooke, M. C., P. N. Francis, S. Millington, R. Saunders and C. Witham (2014), Detection of the Grímsvötn 2011 volcanic eruption plumes using infrared satellite measurements, *Atmospheric Science Letters*, in press, doi: 10.1002/asl2.506

Denlinger, R. P., M. Pavolonis and J. Sieglaff (2012), A robust method to forecast volcanic ash clouds, *J. Geophys. Res.*, *117*, D13208, doi:10.1029/2012JD017732.

Devenish B. J., P. N. Francis, B. T. Johnson, R. S. J. Sparks and D. J. Thomson (2012) Sensitivity analysis of dispersion modeling of volcanic ash from Eyjafjallajökull in May 2010, *J. Geophys. Res.*, *117*, D00U21, doi: 10.1029/2011JD016782

© Crown Copyright 2015

Devenish, B. J. (2013), Using simple plume models to refine the source mass flux of volcanic eruptions according to atmospheric conditions, *J. Volcanol. and Geotherm. Res.*, *256*, 118-127, doi:10.1016/j.volgeores.2013.02.015.

Eckhardt, S., A. J. Prata, P. Seibert, K. Stebel and A. Stohl (2008), Estimation of the vertical profile of sulfur dioxide injection into the atmosphere by a volcanic eruption using satellite column measurements and inverse transport modeling, *Atmos. Chem. Phys.*, *8*, 3881-3897.

Francis, P. N., M. C. Cooke and R. W. Saunders (2012), Retrieval of physical properties of volcanic ash using Meteosat: A case study from the 2010 Eyjafjallajökull eruption, *J. Geophys. Res.*, *117*, D00U09, doi:10.1029/2011JD016788.

Gudmundsson, M. T. et al. (2012), Ash generation and distribution from the April- May 2010 eruption of Eyjafjallajökull, Iceland, *Sci. Rep.*, *2*, 572, doi:10.1038/srep00572.

Hobbs, P. V., L. F. Radke, J. H. Lyons, R. J. Ferek, D. J. Coffman and T. J. Casadevall (1991), Airbourne measurements of particle and gas emissions from the 1990 volcanic eruptions of Mount Redoubt, *J. Geophys. Res.*, *96*, 18,735-18,752.

Hocking, J., P. N. Francis and R. Saunders (2011), Cloud detection in Meteosat Second Generation imagery at the Met Office, *Met. Apps.*, *18*, 307-323, doi:10.1002/met.239.

Jones, A., D. Thomson, M. Hort, and B. Devenish (2007), The U.K. Met Office's next generation atmospheric dispersion model, NAME III, in *Air Pollution Modeling and its Applications XVII: Proceedings of the 27th NATO/CCMS International Technical Meeting on Air Pollution Modeling and its Applications*, edited by Borrego, C. and A.-L. Norman, pp. 580-589, Springer, New York.

Kristiansen, N. I. et al. (2012), Performance assessment of a volcanic ash transport model mini-ensemble used for inverse modeling of the 2010 Eyjafjallajökull eruption, *J. Geophys. Res.*, *117*, D00U11, doi:10.1029/2011JD016844.

Manning, A. J., D. B. Ryall and R. G. Derwent (2003), Estimating European emissions of ozone-depleting and greenhouse gases using observations and a modeling back-attribution technique, *J. Geophys. Res.*, *108*(D14), 4405, doi:10.1029/2002JD002312.

Manning, A. J., S. O'Doherty, A. R. Jones, P. G. Simmonds and R. G. Derwent (2011), Estimating UK methane and nitrous oxide emissions from 1990 to 2007 using an inversion modeling approach, *J. Geophys. Res.*, *116*, D02305, doi:10.1029/2010JD014763.

Manning, A. J. (2011), The challenge of estimating regional trace gas emissions from atmospheric observations, *Phil. Trans. R. Soc. A*, *369*, 1943-1954, doi:10.1098/rsta.2010.0321.

Mastin, L. G. (2007), A user-friendly one-dimensional model for wet volcanic plumes, *Geochem. Geophys. Geosyst.*, *8*, Q03014, doi:10.1029/2006GC001455.

© Crown Copyright 2015

Mastin, L. G. et al. (2009), A multidisciplinary effort to assign realistic source parameters to models of volcanic ash-cloud transport and dispersion during eruptions, *J. Volcanol. and Geotherm. Res.*, *186*, 10-21.

Marzano, F. S., E. Picciotti, M. Montopoli and G. Vulpiani. (2013), Inside volcanic ash clouds: Remote sensing of ash plumes using microwave weather radars, *Bull. Amer. Meteor. Soc.*, *94*, 1567-1586, doi:10.1175/BAMS-D-11-00160.1

Menke, W., (1976), Geophysical Data Analysis: Discrete Inverse Theory, Academic Press, San Diego.

Petersen, G. N. (2010), A short meterological overview of the Eyjafjallajökull eruption 14 April–23 May 2010, *Weather*, *65*, 203-207

Petersen, G. N., H. Bjornsson and P. Arason (2012a), The impact of the atmosphere on the Eyjafjallajökull 2010 eruption plume, *J. Geophys. Res.*, *117*, D00U07, doi:10.1029/2011JD016762.

Petersen, G. N., H. Bjornsson, P. Arason and S. von Löwis (2012b), Two weather radar time series of the altitude of the volcanic plume during the May 2011 eruption of Grímsvötn, Iceland, *Earth Syst. Sci. Data*, *4*, 121-127, doi:10.5194/essd-4/121-2012.

Press, W. H., S. A. Teukolsky, W. T. Vetterling and B. P. Flanner (1992), Numerical Recipes in Fortran: The Art of Scientific Computing, 2nd ed., Cambridge Univ. Press, New York.

Ripepe, M., C. Bonadonna, A. Folch, D. Delle Donne, G. Lacanna, E. Marchetti and A. Höskuldsson (2013), Ash-plume dynamics and eruption source parameters by infrasound and thermal imagery: The 2010 Eyjafjallajökull eruption, *Earth and Planetary Science Letters*, *366*, 112-121, doi:10.1016/j.epsl.2013.02.005.

Rodgers C. D., (1976), Retrieval of atmospheric temperature and composition from remote measurements of thermal radiation, *Rev. Geophys. and Space Phys.*, *14*, 609-624, (1976).

Schmehl, K. J., S. E. Haupt and M. Pavolonis (2011), A genetic algorithm variational approach to data assimilation and application to volcanic emissions, *Pure Appl. Geophys.*, doi: 10.1007/s00024-011-0385-0.

Seibert, P., N. I. Kristiansen, A. Richter, S. Eckhardt, A. J. Prata and A. Stohl (2011), Uncertainties in the inverse modelling of sulphur dioxide eruption profiles, Geomatics, *Natural Hazards and Risk*, *2*, 201-216, doi:10.1080/19475705.2011.590533.

Sparks R. J. S., M. I. Bursik, S. N. Carey, J. S. Gilbert, L. S. Glaze, H. Sigurdsson and A. W. Woods (1997), Volcanic Plumes, John Wiley, Chichester, U.K.

Stohl, A. et al. (2011), Determination of time- and height-resolved volcanic ash emissions and their use for quantitative ash dispersion modeling: the 2010 Eyjafjallajökull eruption, *Atmos. Chem. Phys.*, *11*, 4333-4351, doi:10.5194/acp-11-4333-2011.

© Crown Copyright 2015

Tarantola A., (2005), Inverse Problem Theory and Methods for Model Parameter Estimation, Siam, Philadelphia.

Webster, H. N. et al. (2012), Operational prediction of ash concentrations in the distal volcanic cloud from the 2010 Eyjafjallajökull eruption, *J. Geophys. Res.*, *117*, D00U08, doi:10.1029/2011JD016790.

Woodhouse, M. J., A. J. Hogg, J. C. Phillips and R. S. J. Sparks (2013), Interaction between volcanic plumes and wind during the 2010 Eyjafjallajökull eruption, Iceland, *J. Geophys. Res. Solid Earth*, *118*, 92-109, doi:10.1029/2012JB009592.

Yee E., (2008), Theory for Reconstruction of an Unknown Number of Contaminant Sources using Probabilistic Inference, *Boundary-Layer Meteorol.*, *127*, 359-394, doi:10.1007/s10546-008-9270-5.

© Crown Copyright 2015

This page is intentionally left blank

© Crown Copyright 2015

Met Office	Tel: 0370 900 0100
FitzRoy Road, Exeter	Fax: 0370 900 5050
Devon, EX1 3PB	enquiries@metoffice.gov.uk
UK	www.metoffice.gov.uk

Produced with the Met Office LaTeX template v2.0.0